Frequency preference and attention effects across cortical depths in the human primary auditory cortex

Federico De Martino[a,b,1], Michelle Moerel[b], Kamil Ugurbil[b], Rainer Goebel[a,c], Essa Yacoub[b], and Elia Formisano[a,d]

[a]Department of Cognitive Neurosciences, Faculty of Psychology and Neuroscience, Maastricht University, 6229 ER Maastricht, The Netherlands; [b]Center for Magnetic Resonance Research, Department of Radiology, University of Minnesota, Minneapolis, MN 55455; [c]Department of Neuroimaging and Neuromodeling, Netherlands Institute for Neuroscience, 1105 BA Amsterdam, The Netherlands; and [d]Maastricht Center for Systems Biology (MaCSBio), Maastricht University, 6229 ER, Maastricht, The Netherlands

Edited by Dale Purves, Duke University, Durham, NC, and approved November 17, 2015 (received for review April 17, 2015)

Columnar arrangements of neurons with similar preference have been suggested as the fundamental processing units of the cerebral cortex. Within these columnar arrangements, feed-forward information enters at middle cortical layers whereas feedback information arrives at superficial and deep layers. This interplay of feed-forward and feedback processing is at the core of perception and behavior. Here we provide in vivo evidence consistent with a columnar organization of the processing of sound frequency in the human auditory cortex. We measure submillimeter functional responses to sound frequency sweeps at high magnetic fields (7 tesla) and show that frequency preference is stable through cortical depth in primary auditory cortex. Furthermore, we demonstrate that—in this highly columnar cortex—task demands sharpen the frequency tuning in superficial cortical layers more than in middle or deep layers. These findings are pivotal to understanding mechanisms of neural information processing and flow during the active perception of sounds.

columns | tonotopy | fMRI | 7-Tesla | depth-dependent

Auditory perception starts in our ears, where hair cells at different places in the cochlea respond to different sound frequencies. The spatially ordered arrangement of neural responses to frequencies (tonotopy) that arises from this transduction mechanism is preserved in subcortical (1, 2) and cortical stages of processing, where neuronal populations form multiple tonotopic maps (3, 4). At the cortical level, tonotopic maps describe systematic changes along the surface. In the orthogonal direction (i.e., perpendicular to the cortical surface), aggregates of neurons with parallel axons have been reported (5, 6). These anatomical observations of cortical microcolumns inspired invasive electrophysiological investigations in cats (7), demonstrating that frequency preference is constant across cortical depth (i.e., frequency columns). Since this early study, frequency columns have been observed in a variety of animals (3, 8–10), and a columnar organization has been suggested for other acoustic properties (10, 11). Despite this anatomical and physiological evidence from animal models, the role of cortical columns in auditory perception is not understood (6, 12, 13). To unravel intracolumnar computations, it is of fundamental importance to analyze the transformation of information across cortical depths. Differences in cell types and in patterns of input and output projections suggest a distinct role of cortical layers in neural information processing (5). In particular, behavioral demands and ongoing brain states can modulate the functional properties of layer 2/3 neurons, suggesting that supragranular neuronal populations may be of fundamental relevance for the processing of sensory information in a context-dependent manner (14). Recordings in the primary auditory cortex of animals have shown differences across layers in response latency (15, 16), in frequency selectivity (i.e., tuning width) (8, 16), and in the complexity of neuronal preference to acoustic information (i.e., receptive field) (17). However, the reports are not concordant across species. Moreover, most of the knowledge regarding auditory columnar processing has been obtained in anesthetized animals, making its relation to human behavior unclear.

To date, there is no functional evidence for a columnar organization and for the layer-dependent processing of sound frequency in the human auditory cortex from either invasive or noninvasive recordings. In this study, we address this question noninvasively using high magnetic field (7 tesla) functional magnetic resonance imaging (fMRI) at high spatial resolution and specificity (18, 19). We acquired functional images in the primary auditory cortex (PAC) of five healthy volunteers and estimated the best frequency (BF) responses voxel-by-voxel. Then, by analyzing the 3D spatial variations of these responses, we identified the PAC regions with a stable arrangement of BF across cortical depths. The term "column" has been used with multiple meanings in the past (13). Here, we refer to columnar region as the cortical region where the variation of frequency with depth is significantly smaller compared with the frequency variation orthogonal to depth (i.e., across the surface) (*SI Text*). Further, we examined the functional differences across cortical layers by estimating the cortical depth-dependent changes in frequency tuning during an auditory and a control visual task. We hypothesized that additional top-down processing engaged by the auditory task would modulate the frequency tuning of fMRI responses in the PAC in a cortical depth-dependent manner. Finally, we simulated how the observed changes of frequency tuning across layers and tasks may result in behaviorally relevant changes of neuronal population-based sound representations.

Significance

To the best of our knowledge, our data provide the first imaging evidence compatible with columnar processing of sound frequency in the human auditory cortex. Our study depicts the human auditory cortex with unprecedented spatial detail and demonstrates the feasibility of acquiring submillimeter functional images outside visual/motor cortices, setting the stage for a wide range of research possibilities. Our results elucidate the role of cortical layers in bottom-up and top-down processing of sounds, and suggest that ongoing behavioral goals shape population-based sound representations especially in superficial layers of A1 columns. These results may inform and improve computational models of auditory cortical processing and may be relevant for understanding neurological conditions that do not yet have an imaging "biomarker" (e.g., tinnitus).

Author contributions: F.D.M., M.M., and E.F. designed research; F.D.M. and E.Y. performed research; F.D.M. and E.F. analyzed data; F.D.M., M.M., K.U., R.G., E.Y., and E.F. wrote the paper; and R.G. developed analysis tools.

The authors declare no conflict of interest.

This article is a PNAS Direct Submission.

Freely available online through the PNAS open access option.

[1]To whom correspondence should be addressed. Email: f.demartino@maastrichtuniversity.nl.

This article contains supporting information online at www.pnas.org/lookup/suppl/doi:10.1073/pnas.1507552112/-/DCSupplemental.

Downloaded at Palestinian Territory, occupied on December 9, 2021

www.manaraa.com

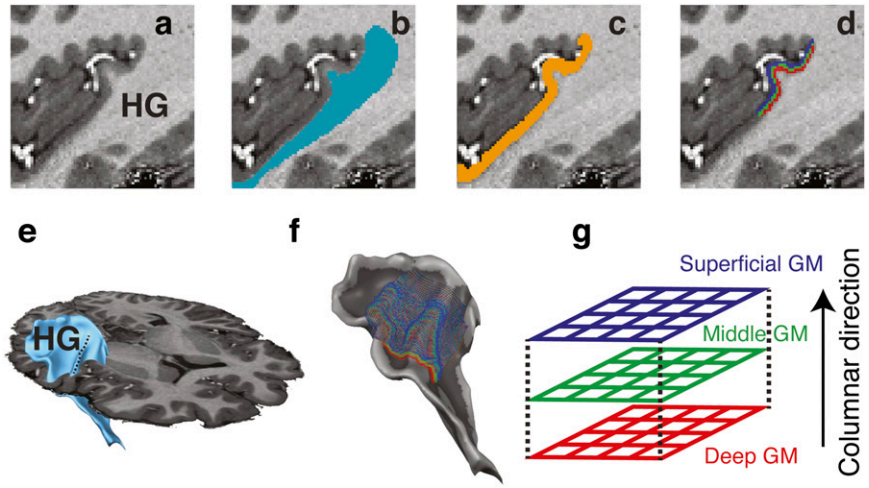

Fig. 1. Illustration of the anatomical segmentation procedure. Anatomical images (*A*) are segmented to identify the white matter (*B*) and gray matter (*C*) in the region of interest [Heschl's gyrus (HG)]. The white/gray matter boundary is used to reconstruct 3D surfaces [blue in *E*; with cortical curvature (light gray, gyrus; dark gray, sulcus) in *F*]. The gray matter region is used to estimate the cortical thickness and obtain regularly spaced grids ($n = 3$; red, green, and blue in *D*, *F*, and *G*) used to evaluate the distribution of functional responses orthogonally to the white/gray matter boundary (i.e., columnar direction).

Results

Initial Identification of the Primary Auditory Cortex and High-Resolution Cortical Sampling. Each volunteer underwent two scanning sessions. In the first session, we acquired a tonotopic functional localizer with a magnetic resonance (MR) acquisition weighted by the effective transversal relaxation time (T_2*-weighted) covering the entire auditory cortex (*SI Text*). Data from these measurements were used to obtain large-scale tonotopic maps and to identify the most likely location of the PAC in each individual. This information was used for positioning the higher resolution functional measurements in the second session. Furthermore, in the first scanning session, we collected high-resolution (0.6 mm isotropic) anatomical data [weighted by: longitudinal relaxation time (T_1-weighted; T_1w); proton density (PD-weighted; PDw); and the effective transversal relaxation time (T_2*-weighted; T_2*w) (in three of the five subjects)]. The combination of T_1w and PDw images resulted in unbiased anatomical images with a good contrast between white matter and gray matter (20). These images were used to obtain a precise definition of the gray matter cortical ribbon (Fig. 1 *A*–*C*) and to derive a 3D surface grid (Fig. 1*D*) enabling the sampling of an fMRI signal at the white/gray matter boundary (Fig. 1*E*) and at different relative cortical depths (Fig. 1*F* and *SI Text*). Points at different cortical depths on the grid follow the direction of maximal cortical thickness variation (Fig. 1*G*). We refer to this direction as the "columnar direction" of the grid. This process was limited to the PAC region as localized by the large-scale tonotopic responses and the high-resolution myelin-related contrast (when available) that was obtained combining T_1w and T_2*w images (21). This procedure resulted in the segmentation of the most medial two thirds of the Heschl's gyrus (HG), in agreement with previous human postmortem anatomical studies of the human PAC (22). In agreement with

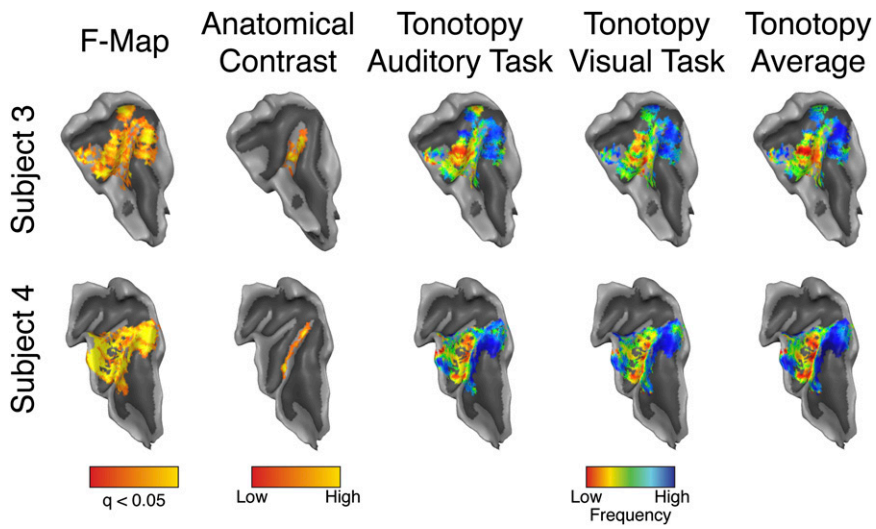

Fig. 2. Single-subject (subject 3 and subject 4) results. The overall response to the sounds (F-Map; FDR corrected $q < 0.05$), intracortical anatomical contrast related to myelin (T1/T2*), and tonotopic maps (auditory task, visual task, and average) are projected on the individual surface reconstruction of the right temporal cortex. For all other subjects, see Fig. S1.

Downloaded at Palestinian Territory, occupied on December 9, 2021
NEUROSCIENCE
www.manaraa.com

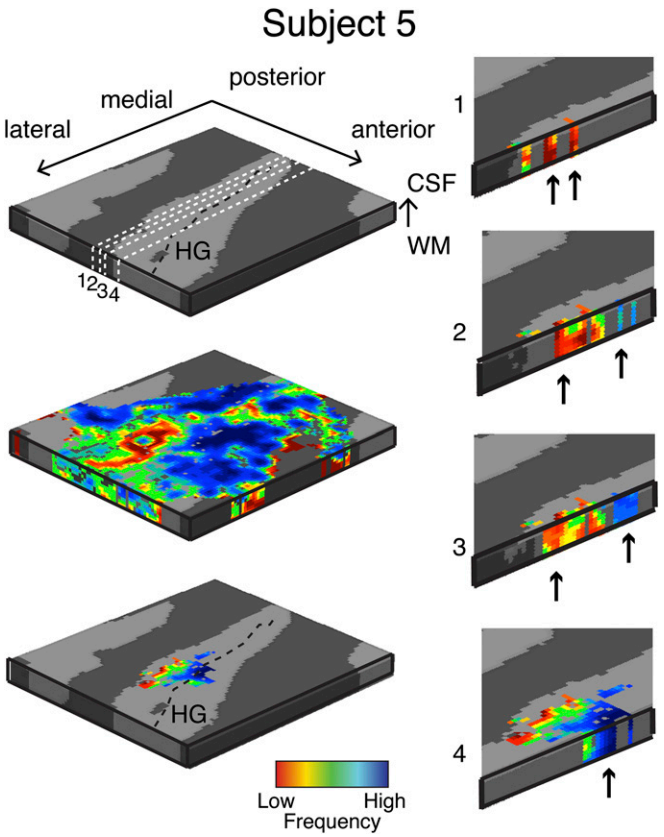

Fig. 3. Single-subject columnar analysis. Tonotopic maps are computed in the grid space of the right HG. Permutation testing is used to determine grid locations with a significant ($P < 0.05$) columnar tonotopic arrangement (*Bottom Left*). (*Right*) Mediolateral cuts through HG and displays the vertical distribution of frequency preference in the columnar region. Arrows indicate example locations with high similarity in BF across cortical depths within the columnar region. For all other subjects, see Figs. S2–S6 and Movies S1–S6.

previous literature (23), we estimated the average cortical thickness of this region of interest to be 2.7 mm (SE across participants = 0.06 mm).

Analysis of Tonotopic Responses Averaged Across Cortical Depths. In the second session, we acquired high-resolution (0.8 mm isotropic) functional images weighted by the transversal relaxation time (T_2-weighted). The high specificity of the T_2-weighted measurements came at the cost of a limited field of view (*SI Text*). In fact, for all our participants, the functional data of the second session were limited to a portion of the right auditory cortex, which was defined, subject-by-subject, based on the data acquired in the first session (*SI Text*). During the measurements, participants listened to frequency sweeps (1,000 ms long, upwards and downward, each spanning a frequency range of 0.4 octaves, exponential change of frequency over time) centered at six frequencies (0.2–6.4 kHz) while fixating on a centrally displayed cross. Per stimulation block, sweeps with one center frequency were presented (eight sweeps per block with an intertrial interval of 1 s). Additionally, within a block, the center frequency of sweeps varied ±0.1 octaves around the block's center frequency. As a result, sweeps across blocks did not overlap in their frequency content. Both upward and downward sweeps were presented. The fixation cross, which was white during silence, changed to either blue or red together with sound presentation. During each run, participants were asked to perform a visual or an auditory task (six blocks per task). In the visual task, subjects had to indicate the color change (blue vs. red) of the fixation cross. In the auditory task, subjects had to indicate the direction of the sweep (up vs. down). In gerbils, learning to categorize up and downward sweeps has been previously shown to induce changes in the neuronal representations at the level of PAC neurons (24), and we hypothesized that our task would also induce measurable effects at the level of neuronal populations in the human PAC.

The functional data were analyzed to estimate the responses to all conditions (six frequencies for each of the two tasks) using a standard general linear model. For a first quality assessment, the data were averaged across depths and projected on the surface boundary between white matter and gray matter. In all subjects, the sounds elicited significant [using a threshold (q) corrected for multiple comparisons using false discovery rate; q(FDR) of <0.05] responses in the right medial two thirds of HG and the adjacent Heschl's sulcus (HS). Furthermore, responses were present in the portions of planum temporale and polare that were included in the acquisition field of view (Fig. 2 and Fig. S1). The voxels' BF was determined as the frequency eliciting the strongest response (4) for the two tasks separately. When examining the spatial layout of BF (averaged across cortical depths) (Fig. 2 and Fig. S1), all subjects showed a mirror-reversed topographical organization of frequency preference (tonotopy) for both tasks. Specifically, a region of low frequency preference was present on HG. Regions preferring higher frequencies were located posteromedially and anterolaterally to HG (4).

Mapping of the Cortical Depth-Dependent Organization for Frequency Processing. After this initial analysis, we investigated whether frequency preference was constant across cortical depths. We sampled the single voxel functional responses to sounds of all six center frequencies in the depth-dependent grid space, independently for the two tasks. For each task, this analysis resulted in frequency response profiles for each grid point in the range (0.2–6.4 kHz). Per task, we estimated each grid point's BF (the frequency eliciting the strongest response) and, using a fitting procedure (*SI Text*), the full width at half maximum (FWHM) of the frequency response for that grid point. We obtained an estimate of tuning width (TW) as the ratio between the grid point's BF and the FWHM. The tonotopic maps at different cortical depths were

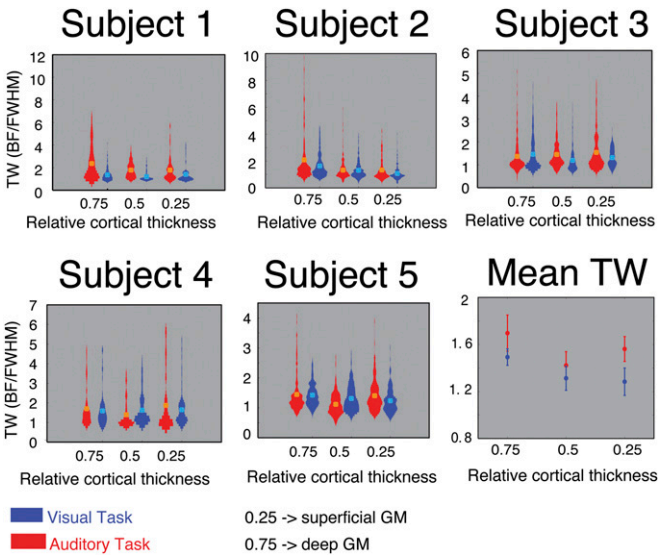

Fig. 4. Task-dependent modulation of tuning width across cortical depths. Single-subject distributions are presented together with subjects' mean TW value (orange and cyan dots). The mean across subjects (*Bottom Right*) is presented together with error bars indicating the SE across subjects. At superficial cortical depths (0.25 relative cortical thickness), TW values were significantly higher for the auditory task compared with the visual task, indicating narrower tuning ($P < 0.05$; paired t test).

Downloaded at Palestinian Territory, occupied on December 9, 2021
www.manaraa.com

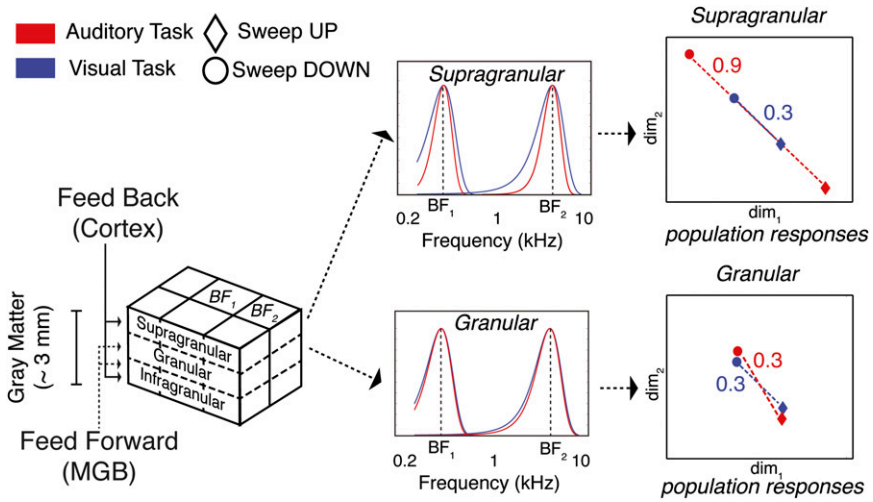

Fig. 5. Effect of frequency tuning width sharpening on the population responses to upward and downward sweeps. The pattern of cortical depth-dependent inputs to a columnar region of primary auditory cortex (5, 40) is summarized on the *Left*. For two different cortical depths (i.e., supragranular and granular), the frequency response of different units is simulated as a Gaussian function with mean equal to the BF and full width at half maximum (FWHM = BF/TW) equal to the value empirically estimated from our fMRI data. The task modulation (red, auditory task; blue, visual task) acts on the TW: i.e., sharpens the frequency response in the supragranular but not in the granular layer. Average responses to upward and downward sweeps (circles and diamonds, respectively) are represented using 2D multidimensional scaling. As a result of the sharpening, the Euclidean distance between upward and downward sweeps during the auditory task increases at the population level in the supragranular layers.

submitted to an analysis that evaluated the gradient of frequency change in three dimensions. From the tonotopic gradient, we obtained a measure of "columnarity" as the ratio between the components of the gradient parallel and orthogonal to the columnar direction (*SI Text*). The ratio R was distributed in the interval (0.0004–1.8) for each individual subject. Across subjects, the average median value of R was 0.2 (SE = 0.02). Values greater than $R = 1$ indicate regions where the tonotopic map varied more along the cortical surface than across cortical depths (the columnar direction). Note that this procedure may underestimate columnarity in regions that present a stable frequency preference within spatially extended patches on the cortical surface. In each subject, we tested for significance of the frequency columnarity ratio with permutation testing (*SI Text*). The analysis was repeated for both tasks, and the regions that, after permutation testing, resulted in a significant ($P < 0.05$ uncorrected) columnarity ratio in at least one of the tasks were selected. We refer to these regions as frequency columns. The average significant threshold of R across our participants was 0.49 (SE = 0.0045). We found such regions in the most medial portion of HG in all subjects (Fig. 3 and Figs. S2–S5). We demonstrated the reliability of these regions by comparing measurements taken several days apart (Fig. S6) and addressing potential confounds of the acquisition (Fig. S7). At lower cortical depths, the columnar region in HG was characterized by high intracortical contrast related to myelin (measured in vivo in three subjects) (Fig. S8), a characteristic of the primary auditory cortex (21, 22).

To quantify the cortical distribution of frequency in highly columnar regions of the PAC, we calculated on each participant's cortical surface the iso-frequency contours corresponding to the maximum frequency and to the frequencies one to four octaves lower. We then measured the cortical area covered by responses spanning one octave (i.e., we calculated the surface area within iso-frequency lines). Averaging across octave intervals and subjects, we obtained an estimate of 16 mm^2 (± 3 mm^2, SE), per octave.

Task- and Layer-Dependent Modulations of Frequency Tuning. Within the identified columnarly organized HG regions, we did not observe significant changes in the overall fMRI response with task. This result is possibly due to the relative simplicity of both tasks: Behavioral performance was of 91% and 92% for the auditory and visual tasks, respectively, with no significant difference across tasks and subjects. Furthermore, frequency preference did not show any significant change across the two tasks. Instead, we observed a narrower tuning width during the auditory task compared with the visual task (Fig. 4). At the group level, the difference was significant ($P < 0.05$, paired t test) at superficial cortical depths only. This finding suggests that a selective refinement of acoustic information occurs within a column and that top-down information relevant to behavior acts primarily in superficial layers and to a lesser degree in deeper layers. In fact, in our experiment, narrower frequency tuning allowed better discrimination at the neuronal population level between upward and downward sweeps. A simulation of tonotopic responses with BF and TW in the ranges obtained with our fMRI responses illustrates this effect (Fig. 5, *Right* and *SI Text*).

Discussion

Our results provide direct evidence of a stable arrangement of frequency preference across depths of the human primary auditory cortex (Fig. 5, *Left*). We analyzed the gradients of frequency preference on the cortical surface and across cortical depth in the right HG and adjacent HS in five healthy volunteers. By doing, so we did not identify single discrete columnar entities, but rather showed that the most medial portion of HG exhibited significantly smaller variability of the population frequency preference in the direction orthogonal to the cortical surface compared with the rest of the imaged field of view. We refer to this region as a highly columnar region of the cortex. The identification of the columnar region in single subjects was remarkably stable across tasks even at several days of separation. Further, the columnar locations exhibited higher cortical contrast related to myelin in deep sections of the cortex, a characteristic of the PAC (22). To achieve high spatial specificity and resolution, our functional (T_2-weighted) scans were acquired with field of view restriction and covered one hemisphere.

The presence of regions with almost constant frequency preference across cortical depth reflects the relevance of frequency processing in these cortical regions, but by itself it does

Downloaded at Palestinian Territory, occupied on December 9, 2021

NEUROSCIENCE

www.manaraa.com

not reveal the nature of the computations that are performed within these regions. To investigate the nature of these computations, we analyzed cortical depth-dependent changes induced by different tasks. Previous literature has shown that fMRI can detect layer-dependent signal changes using both T_2*-weighted and T_2-weighted measurements (25–30). We analyzed the differential changes induced by the auditory and visual tasks on the frequency population tuning and selectivity. We were able to show that population level frequency responses sharpen with cortical depth when attending to the auditory stimuli. These results provide strong evidence that acoustic information processing in primary cortical areas is modulated by task demands, a result that has been debated in the literature (31–34). Further, we demonstrate that attention can selectively improve neural processing of acoustic information within a column by sharpening the receptive field in upper cortical (supragranular) layers (Fig. 5, *Center*). At the neuronal population level, this effect results in increased distance between the responses to upward and downward sweeps (Fig. 5, *Right*). The sharpening of the tuning width may be explained by the task-induced phase reset of frequency-selective neuronal populations, which has been shown to have the most pronounced effects in supragranular auditory layers (35, 36).

Previous animal studies have shown that the shape of receptive fields of primary auditory neurons can be modulated by a detection (37) and discrimination (38) task compared with passive listening. Here, by asking participants to perform either a visual or auditory task, we were able to modulate population frequency responses and observe these changes noninvasively with fMRI. These changes were visible despite the relatively weak manipulation of attention (task performance was 91% and 92% for the auditory and visual task, respectively). The effective relation and relevance to behavior of this mechanism need to be further investigated: e.g., by manipulating parametrically the difficulty of an auditory task.

Our study of frequency preference paves the way for in vivo investigations into the fine-grained representation and processing of acoustic properties in auditory cortex. Using complex stimuli, such as dynamic ripples and natural sounds, it is possible to derive the neuronal population preference to spectrotemporal acoustic properties beyond frequency (39). Together with those stimuli, the methods used here can be exploited to investigate cortical depth stability or laminar variability of neuronal population tuning to other acoustic features, such as spectral and temporal modulations, aural dominance and binaural interaction, and frequency sweep direction (10, 11, 16). Finally, this study provides the basis for investigating neuronal population receptive field changes during increasingly complex auditory and multisensory tasks. Specifically, future studies of auditory feature detection, discrimination, and learning will enable the generalization of the top-down mechanism we uncovered here.

Materials and Methods

Five subjects (median age = 25 y, all females) participated in the study. The subjects had no history of hearing disorder or neurological disease. The Institutional Review Board (IRB) for human subject research at the University of Minnesota granted approval for the study, and procedures followed the principles expressed in the Declaration of Helsinki. Informed consent was obtained from each participant before conducting the experiments.

In a first session, we measured high-resolution ($0.6 \times 0.6 \times 0.6$ mm^3) anatomical images, allowing a precise definition of the gray matter cortical ribbon (20) and the functional activation elicited by amplitude-modulated tones ($n = 5$; with voxel size = $1.5 \times 1.5 \times 1.5$ mm^3) (*SI Text*). These measurements covered the entire right hemisphere of each subject, and the large-scale tonotopic maps obtained from the analysis of these data were used to localize the primary auditory cortex (PAC) individually. Additionally, in three subjects, this information was complemented by the acquisition of high-resolution ($0.6 \times 0.6 \times 0.6$ mm^3) anatomical data whose contrast is related to the myelin content, enabling an anatomical localization of the PAC (21).

Using this individually tailored localization information, in a second session, we zoomed into the functional responses of individuals' right PAC by acquiring high spatial resolution (nominal voxel size = $0.8 \times 0.8 \times 0.8$ mm^3) T_2-weighted functional data. Sounds were blocked with respect to center frequency and were presented in silent gaps between the acquisitions of functional volumes to reduce contamination with the scanner noise. All data analysis was performed at the individual subject level. To evaluate the reproducibility of our results, we asked one of the participants (subject 5) to perform the full experiment a second time at several days distance and repeated the analysis independently for the two datasets.

ACKNOWLEDGMENTS. This work was supported in part by Biomedical Technology Resource Centers, National Institute of Biomedical Imaging and Bioengineering Grant P41 EB015894. The 7-T magnet purchase was funded in part by the W. M. Keck Foundation, National Science Foundation Grant DBI-9907842, and National Institutes of Health Grant S10 RR1395. R.G. was supported by European Research Council Grant ERC-2010-AdG, 269853. E.F. was funded by The Netherlands Organisation for Scientific Research (NWO) VICI Grant 453-12-002. F.D.M. was funded by NWO VIDI Grant 864-13-012. M.M. was funded by NWO Rubicon Grant 446-12-010.

1. Merzenich MM, Reid MD (1974) Representation of the cochlea within the inferior colliculus of the cat. *Brain Res* 77(3):397–415.
2. De Martino F, et al. (2013) Spatial organization of frequency preference and selectivity in the human inferior colliculus. *Nat Commun* 4:1386.
3. Merzenich MM, Brugge JF (1973) Representation of the cochlear partition of the superior temporal plane of the macaque monkey. *Brain Res* 50(2):275–296.
4. Formisano E, et al. (2003) Mirror-symmetric tonotopic maps in human primary auditory cortex. *Neuron* 40(4):859–869.
5. Winer JA, Schreiner CE, eds (2009) *The Auditory Cortex* (Springer, New York).
6. Linden JF, Schreiner CE (2003) Columnar transformations in auditory cortex? A comparison to visual and somatosensory cortices. *Cereb Cortex* 13(1):83–89.
7. Abeles M, Goldstein MH, Jr (1970) Functional architecture in cat primary auditory cortex: Columnar organization and organization according to depth. *J Neurophysiol* 33(1):172–187.
8. Sugimoto S, Sakurada M, Horikawa J, Taniguchi I (1997) The columnar and layer-specific response properties of neurons in the primary auditory cortex of Mongolian gerbils. *Hear Res* 112(1-2):175–185.
9. Shen JX, Xu ZM, Yao YD (1999) Evidence for columnar organization in the auditory cortex of the mouse. *Hear Res* 137(1-2):174–177.
10. Shamma SA, Fleshman JW, Wiser PR, Versnel H (1993) Organization of response areas in ferret primary auditory cortex. *J Neurophysiol* 69(2):367–383.
11. Imig TJ, Adrián HO (1977) Binaural columns in the primary field (A1) of cat auditory cortex. *Brain Res* 138(2):241–257.
12. Horton JC, Adams DL (2005) The cortical column: A structure without a function. *Philos Trans R Soc Lond B Biol Sci* 360(1456):837–862.
13. Rakic P (2008) Confusing cortical columns. *Proc Natl Acad Sci USA* 105(34): 12099–12100.
14. Petersen CC, Crochet S (2013) Synaptic computation and sensory processing in neocortical layer 2/3. *Neuron* 78(1):28–48.
15. Phillips DP, Irvine DR (1981) Responses of single neurons in physiologically defined primary auditory cortex (AI) of the cat: Frequency tuning and responses to intensity. *J Neurophysiol* 45(1):48–58.
16. Atencio CA, Schreiner CE (2010) Laminar diversity of dynamic sound processing in cat primary auditory cortex. *J Neurophysiol* 103(1):192–205.
17. Atencio CA, Sharpee TO, Schreiner CE (2009) Hierarchical computation in the canonical auditory cortical circuit. *Proc Natl Acad Sci USA* 106(51):21894–21899.
18. Yacoub E, Harel N, Ugurbil K (2008) High-field fMRI unveils orientation columns in humans. *Proc Natl Acad Sci USA* 105(30):10607–10612.
19. Yacoub E, Shmuel A, Logothetis N, Uğurbil K (2007) Robust detection of ocular dominance columns in humans using Hahn Spin Echo BOLD functional MRI at 7 Tesla. *Neuroimage* 37(4):1161–1177.
20. Van de Moortele P-F, et al. (2009) T1 weighted brain images at 7 Tesla unbiased for Proton Density, T2* contrast and RF coil receive B1 sensitivity with simultaneous vessel visualization. *Neuroimage* 46(2):432–446.
21. De Martino F, et al. (2015) High-resolution mapping of myeloarchitecture in vivo: Localization of auditory areas in the human brain. *Cereb Cortex* 25(10):3394–3405.
22. Hackett TA, Preuss TM, Kaas JH (2001) Architectonic identification of the core region in auditory cortex of macaques, chimpanzees, and humans. *J Comp Neurol* 441(3):197–222.
23. Meyer M, Liem F, Hirsiger S, Jäncke L, Hänggi J (2014) Cortical surface area and cortical thickness demonstrate differential structural asymmetry in auditory-related areas of the human cortex. *Cereb Cortex* 24(10):2541–2552.
24. Ohl FW, Scheich H, Freeman WJ (2001) Change in pattern of ongoing cortical activity with auditory category learning. *Nature* 412(6848):733–736.
25. Polimeni JR, Fischl B, Greve DN, Wald LL (2010) Laminar analysis of 7T BOLD using an imposed spatial activation pattern in human V1. *Neuroimage* 52(4):1334–1346.

Downloaded at Palestinian Territory, occupied on December 9, 2021
www.manaraa.com

26. Ress D, Glover GH, Liu J, Wandell B (2007) Laminar profiles of functional activity in the human brain. *Neuroimage* 34(1):74–84.
27. Koopmans PJ, Barth M, Norris DG (2010) Layer-specific BOLD activation in human V1. *Hum Brain Mapp* 31(9):1297–1304.
28. Koopmans PJ, Barth M, Orzada S, Norris DG (2011) Multi-echo fMRI of the cortical laminae in humans at 7 T. *Neuroimage* 56(3):1276–1285.
29. Siero JCW, Petridou N, Hoogduin H, Luijten PR, Ramsey NF (2011) Cortical depth-dependent temporal dynamics of the BOLD response in the human brain. *J Cereb Blood Flow Metab* 31(10):1999–2008.
30. De Martino F, et al. (2013) Cortical depth dependent functional responses in humans at 7T: Improved specificity with 3D GRASE. *PLoS One* 8(3):e60514.
31. Petkov CI, et al. (2004) Attentional modulation of human auditory cortex. *Nat Neurosci* 7(6):658–663.
32. Da Costa S, van der Zwaag W, Miller LM, Clarke S, Saenz M (2013) Tuning in to sound: Frequency-selective attentional filter in human primary auditory cortex. *J Neurosci* 33(5):1858–1863.
33. Oh J, Kwon JH, Yang PS, Jeong J (2013) Auditory imagery modulates frequency-specific areas in the human auditory cortex. *J Cogn Neurosci* 25(2):175–187.
34. Paltoglou AE, Sumner CJ, Hall DA (2009) Examining the role of frequency specificity in the enhancement and suppression of human cortical activity by auditory selective attention. *Hear Res* 257(1-2):106–118.
35. Lakatos P, et al. (2009) The leading sense: Supramodal control of neurophysiological context by attention. *Neuron* 64(3):419–430.
36. O'Connell MN, Barczak A, Schroeder CE, Lakatos P (2014) Layer specific sharpening of frequency tuning by selective attention in primary auditory cortex. *J Neurosci* 34(49): 16496–16508.
37. Fritz J, Shamma S, Elhilali M, Klein D (2003) Rapid task-related plasticity of spectrotemporal receptive fields in primary auditory cortex. *Nat Neurosci* 6(11): 1216–1223.
38. Fritz JB, Elhilali M, Shamma SA (2005) Differential dynamic plasticity of A1 receptive fields during multiple spectral tasks. *J Neurosci* 25(33):7623–7635.
39. Santoro R, et al. (2014) Encoding of natural sounds at multiple spectral and temporal resolutions in the human auditory cortex. *PLOS Comput Biol* 10(1):e1003412.
40. Constantinople CM, Bruno RM (2013) Deep cortical layers are activated directly by thalamus. *Science* 340(6140):1591–1594.
41. Oshio K, Feinberg DA (1991) GRASE (Gradient- and spin-echo) imaging: A novel fast MRI technique. *Magn Reson Med* 20(2):344–349.
42. Vaughan JT, et al. (2001) 7T vs. 4T: RF power, homogeneity, and signal-to-noise comparison in head images. *Magn Reson Med* 46(1):24–30.
43. Uğurbil K, et al. (2003) Ultrahigh field magnetic resonance imaging and spectroscopy. *Magn Reson Imaging* 21(10):1263–1281.
44. Ogawa S, et al. (1992) Intrinsic signal changes accompanying sensory stimulation: Functional brain mapping with magnetic resonance imaging. *Proc Natl Acad Sci USA* 89(13):5951–5955.
45. Yacoub E, et al. (2001) Imaging brain function in humans at 7 Tesla. *Magn Reson Med* 45(4):588–594.
46. Zhao F, Wang P, Hendrich K, Ugurbil K, Kim S-G (2006) Cortical layer-dependent BOLD and CBV responses measured by spin-echo and gradient-echo fMRI: Insights into hemodynamic regulation. *Neuroimage* 30(4):1149–1160.
47. Harel N, Lin J, Moeller S, Ugurbil K, Yacoub E (2006) Combined imaging-histological study of cortical laminar specificity of fMRI signals. *Neuroimage* 29(3):879–887.
48. Uludağ K, Müller-Bierl B, Uğurbil K (2009) An integrative model for neuronal activity-induced signal changes for gradient and spin echo functional imaging. *Neuroimage* 48(1):150–165.
49. Yacoub E, Van De Moortele P-F, Shmuel A, Uğurbil K (2005) Signal and noise characteristics of Hahn SE and GE BOLD fMRI at 7 T in humans. *Neuroimage* 24(3): 738–750.
50. Goense JBM, Zappe A-C, Logothetis NK (2007) High-resolution fMRI of macaque V1. *Magn Reson Imaging* 25(6):740–747.
51. Goense JBM, Logothetis NK (2006) Laminar specificity in monkey V1 using high-resolution SE-fMRI. *Magn Reson Imaging* 24(4):381–392.
52. Norris DG (2012) Spin-echo fMRI: The poor relation? *Neuroimage* 62(2):1109–1115.
53. Feinberg DA, Harel N, Ramanna S, Ugurbil K, Yacoub E (2008) Sub-millimeter single-shot 3D GRASE with inner volume selection for T2-weighted fMRI applications at 7T. *Proc Int Soc Mag Reson Med* 16:2373.
54. Zimmermann J, et al. (2011) Mapping the organization of axis of motion selective features in human area MT using high-field fMRI. *PLoS One* 6(12):e28716.
55. Olman C, et al. (2012) Layer-specific fMRI reflect different nuronal computations at different depths in human V1. *PLoS ONE* 7(3):e32536.
56. Baumann S, Petkov CI, Griffiths TD (2013) A unified framework for the organization of the primate auditory cortex. *Front Syst Neurosci* 7:11.
57. Moerel M, De Martino F, Formisano E (2014) An anatomical and functional topography of human auditory cortical areas. *Front Neurosci* 8:225.
58. Sled JG, Zijdenbos AP, Evans AC (1997) A comparison of retrospective intensity non-uniformity correction methods for MRI. *Information Processing in Medical*, Imaging Lecture Notes in Computer Science (Springer, Berlin), Vol 1230, pp 459–464.
59. Jones SE, Buchbinder BR, Aharon I (2000) Three-dimensional mapping of cortical thickness using Laplace's equation. *Hum Brain Mapp* 11(1):12–32.
60. Glasser MF, Goyal MS, Preuss TM, Raichle ME, Van Essen DC (2014) Trends and properties of human cerebral cortex: Correlations with cortical myelin content. *Neuroimage* 93(Pt 2):165–175.

Downloaded at Palestinian Territory, occupied on December 9, 2021

www.manaraa.com